

Typical density profile for warm dark matter haloes

Jordi Viñas^{*}, Eduard Salvador-Solé and Alberto Manrique

Institut de Ciències del Cosmos, Universitat de Barcelona (UB–IEEC), Martí i Franquès 1, E-08028 Barcelona, Spain

15 February 2012

ABSTRACT

Using the model recently developed by Salvador-Solé et al. (2012), we derive the typical spherically averaged halo density profile from the power-spectrum of density perturbations in the concordant Λ warm dark matter (WDM) cosmology with 2 keV non-thermal sterile neutrinos. This allows us to analyse separately the effects on the density profile at small radii of the spectrum cutoff caused by free-streaming and the bound in the fine-grained phase-space density, both due to the non-negligible particle velocities at decoupling.

Key words: cosmology: theory — dark matter — dark matter: haloes

1 INTRODUCTION

Matter in the Universe is predominantly dark and clustered in haloes that grow through mergers and accretion. The concordant Λ , dissipationless collisionless, cold dark matter (CDM) model recovers the observed large-scale properties of the Universe: it correctly predicts the microwave background radiation anisotropies (Komatsu et al. 2011) and galaxy clustering (Cole et al. 2005). However, some problems arise in the small-scale regime: it predicts excessive substructure with a deficient distribution of maximum circular velocities (Klypin et al. 1999; Moore et al. 1999; Boylan-Kolchin et al. 2011) and a sharp central cusp in the halo density profile, apparently in conflict with the profiles observed in dwarf galaxies (Goerdt et al. 2006). While the disagreement in the satellite abundance and characteristics might be explained through the inhibition of star formation owing to several baryonic feedback processes, the cusp problem seems to be insurmountable.

Several modifications of the Λ CDM model have been proposed that, keeping its right predictions at large scales, may improve those compromised at small scales. This includes the cosmological models dominated by self-interacting dark matter (Spergel & Steinhardt 2000; Kaplinghat et al. 2000; Bento et al. 2000) and dissipationless collisionless warm dark matter (WDM). The best candidate particles in the latter category of dark matter are the gravitino (Ellis et al. 1984; Hogan & Dalcanton 2000; Kaplinghat et al. 2005; Gorbunov et al. 2008) and non-thermal sterile neutrino (Dodelson & Widrow 1994; Hogan & Dalcanton 2000; Shaposhnikov & Tkachev 2006). Specifically, the case of light sterile neutrinos is being attracting growing interest as this kind of particles is naturally foreseen in a minimal extension of the Standard Model.

The non-negligible WDM particle velocities at decoupling introduce a cutoff in the power-spectrum due to free-streaming and, at the same time, a bound in the fine-grained phase-space density. The former effect should inhibit the formation of haloes below the corresponding free-streaming mass scale, M_{fs} , which would presumably produce a central core in the subsequent generations of more massive haloes. The latter should translate into an upper bound in the coarse-grained phase-space density of haloes resulting from virialisation, which could also lead to the formation of a core. Both aspects depend, however, critically on the poorly known way haloes fix their density profiles.

In fact, N -body simulations do not confirm such expectations: WDM haloes show similar density profiles as CDM haloes (e.g. Colombi et al. 1996; Colín et al. 2000; Knebe et al. 2002; Wang & White 2009; Schneider et al. 2011). Only a small hint towards increased scaled radii has been found (Bode et al. 2001), although the opposite trend, namely a slight inflection towards sharper density profile at small radii, has also been reported (Colín et al. 2008). The situation is further complicated by the fact that simulations of WDM cosmologies find a substantial amount of haloes with masses considerably smaller than M_{fs} . These low-mass haloes may be spurious due to the effects of the periodical grid used in simulations (Wang & White 2007), but even so they could affect the density profile of more massive haloes formed from their mergers and accretion. In addition, the expected size of the core (if any) for the relevant WDM particle masses is close to the resolution of current simulations, which might explain the negative results above.

All these uncertainties would disappear if the halo density profile could be inferred analytically down to arbitrarily small radii directly from the power-spectrum of density perturbations. Salvador-Solé et al. (2012, hereafter SVMS) have recently built a model for the inner structure of dis-

^{*} E-mail: jvinas@am.ub.es

sipationless collisionless dark matter haloes in bottom-up hierarchical cosmologies¹ that fills this gap.

In the present Letter, we apply the SVMS model to the Λ WDM cosmology that results from 2 keV non-thermal sterile neutrinos, i.e. the minimum mass compatible with the Lyman- α forest (Boyersky et al. 2009). The corresponding linear power-spectrum is given by (Viel et al. 2005)

$$P_{\text{WDM}}(k) = T_{\text{fs}}^2(k) P_{\text{CDM}}(k), \quad (1)$$

where $P_{\text{CDM}}(k)$, is the linear power-spectrum for the wmap7 concordance Λ CDM cosmology (Komatsu et al. 2011) and $T_{\text{fs}}(k)$ is the ‘transfer’ function, well-fitted by

$$T_{\text{fs}}(k) = [1 + (\alpha k)^{2\mu}]^{-5/\mu}, \quad (2)$$

with $\mu = 1.12$ and

$$\alpha = 0.07 \left(\frac{h}{0.7} \right)^{0.22} \left(\frac{m_{\text{WDM}}}{1 \text{ keV}} \right)^{-1.11} \left(\frac{\Omega_{\text{WDM}}}{0.25} \right)^{0.11} \text{ Mpc}, \quad (3)$$

being h the current value of the Hubble parameter in units of $100 \text{ km s}^{-1} \text{ Mpc}^{-1}$, m_{WDM} the WDM particle mass and Ω_{WDM} the WDM density parameter. For the cosmology here considered this yields $\alpha = 0.032 \text{ Mpc}$. By comparing the halo density profile predicted in this WDM cosmology with that found in the underlying CDM one, we analyse separately the effects of the spectrum cutoff and the initial velocity dispersion. In Section 2, we describe the method used, in Section 3, to infer the density profile for halo seeds and, in Section 4, the density profile for haloes themselves. We conclude in Section 5.

2 THE MODEL

In any *bottom-up hierarchical cosmology*, haloes form through either major mergers or smooth accretion (including minor mergers). Both processes involve the virialisation of the halo each time the mass increases. As virialisation is a relaxation process yielding the memory loss of the past history, the density profile for haloes having suffered major mergers is indistinguishable from that for haloes having grown by pure accretion (PA; see SVMS for a complete rigorous explanation). Consequently, we have the right to concentrate in this latter kind of haloes.

As shown in SVMS, *accreting dissipationless collisionless dark matter haloes* evolve from the inside out, keeping their instantaneous inner structure unaltered. In these conditions, the radius of the sphere with mass M is exactly equal to its virial radius,

$$r = \frac{3GM^2}{10|E_p(M)|}, \quad (4)$$

where $E_p(M)$ is the total energy of the sphere encompassing the same mass M in the (spherically averaged) seed, namely a peak in the primordial random Gaussian density field filtered at the scale M . Thus, provided the energy distribution in peaks is known, equation (4) is an implicit equation for the halo mass profile $M(r)$.

¹ In WDM cosmologies there is a minimum halo mass, but haloes still form hierarchically through the merger of less massive objects previously formed and their accretion of diffuse matter.

We must remark that equation (4) is only valid provided the isodensity contours in the seed reach turnaround without shell-crossing at increasingly larger radii (see SVMS). This is certainly the case when the initial peculiar velocities are negligible, as those induced by random Gaussian density fluctuations, and the seed expands in linear regime. However, if there are peculiar velocities of non-gravitational origin such that they dominate the dynamics at small enough scales, then the system may not expand in linear regime and there may be shell-crossing before turnaround, so equation (4) may no more be valid. We will come back to this possibility in Section 4.

In the parametric form, $E_p(M)$ is given by the total energy in the sphere with radius R_p centred at the peak,

$$E_p(R_p) = 4\pi \int_0^{R_p} dr_p r_p^2 \langle \rho_p \rangle(r_p) \times \left\{ \frac{[H(t_i)r_p - v_p(r_p)]^2}{2} + \frac{\sigma_{\text{DM}}^2(t_i)}{2} - \frac{GM(r_p)}{r_p} \right\}, \quad (5)$$

together with the mass of the sphere,

$$M = 4\pi \int_0^{R_p} dr_p r_p^2 \langle \rho_p \rangle(r_p), \quad (6)$$

where $\langle \rho_p \rangle(r_p)$ is the spherically averaged (unconvolved) protohalo density profile, $M(r_p)$ the corresponding mass profile, $H(t_i)$ the Hubble parameter at the cosmic time t_i when the seed is considered, $\sigma_{\text{DM}}(t_i)$ the adiabatically evolved particle velocity dispersion of non-gravitational origin² and $v_p(r_p)$ is, to leading order in the deviations from spherical symmetry, the peculiar velocity at the radius r_p in the seed owing to the inner mass excess³,

$$v_p(r_p) = -\frac{2G[M(r_p) - 4\pi r_p^3 \bar{\rho}(t_i)/3]}{3H(t_i)r_p^2}, \quad (7)$$

being $\bar{\rho}(t_i)$ the mean cosmic density at t_i .

The steps to be followed are thus the following ones: 1) determination of the spherically averaged protohalo density profile $\langle \rho_p \rangle(r_p)$ from the linear power-spectrum of the cosmology considered (see Sec. 3), 2) calculation from it of the energy distribution $E_p(M)$ (eqs. [5]–[6]), and 3) derivation of the typical halo mass profile $M(r)$ by inversion of equation (4), and of the typical spherically averaged halo density profile, through the trivial relation

$$\langle \rho \rangle(r) = \frac{1}{4\pi r^2} \frac{dM}{dr}. \quad (8)$$

3 PROTOHALO DENSITY PROFILE

In PA, every halo ancestor along the continuous series ending at the halo with M at t also arises from one peak in the random density field at t_i , filtered at the mass scale of the ancestor. Thus, the value at the origin ($r_p = 0$) of the convolution of the spherically averaged density contrast profile for the protohalo, $\langle \delta_p \rangle(r_p)$, by a Gaussian window of every

² The velocity dispersion due to random density fluctuations is several orders of magnitude smaller and can be safely neglected (see SVMS).

³ In equation (7) we have taken into account that the cosmic virial factor $f(\Omega) \approx \Omega^{0.1}$ is at t_i very approximately equal to one.

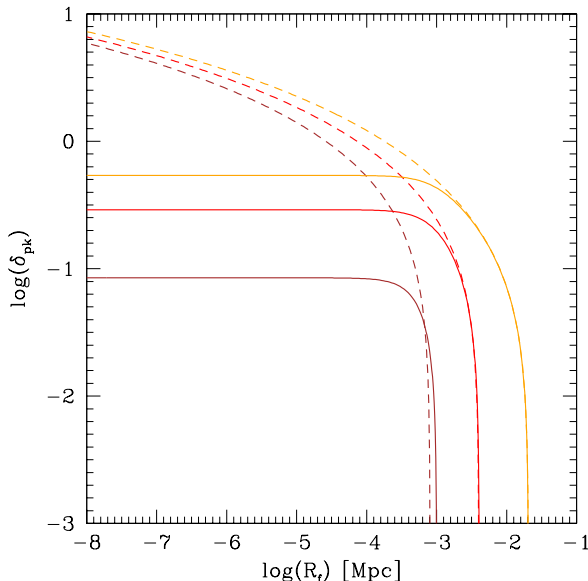


Figure 1. Central density contrast of peaks in the filtered density field at $z = 100$ giving rise by PA to current haloes with masses equal to $10^9 M_\odot$ (brown lines), $10^{11} M_\odot$ (red lines) and $10^{13} M_\odot$ (orange lines) as a function of the Gaussian filtering radius R_f . The different lines correspond to the Λ CDM concordance cosmology (dashed lines) and the Λ WDM cosmology with 2 keV sterile neutrinos (solid lines). Radii are in physical units.

radius R_f must be equal to the density contrast of a peak equally convolved,

$$\delta_{pk}(R_f) = \frac{4\pi}{(2\pi)^{3/2} R_f^3} \int_0^\infty dr_p r_p^2 \delta_p(r_p) e^{-\frac{1}{2} \left(\frac{r_p}{R_f}\right)^2}. \quad (9)$$

Therefore, provided the peak trajectory, $\delta_{pk}(R_f)$, associated with the accreting halo were known, equation (9) could be seen as a Fredholm integral equation of first kind for $\langle \delta_p \rangle(r_p)$. Such an equation can be solved (see SVMS for details), so this would lead to the density profile $\langle \rho_p(r_p) \rangle$ for the seed of the halo evolving by PA.

Furthermore, in any *random Gaussian density field*, the typical peak trajectory $\delta_{pk}(R_f)$ leading to a purely accreting halo with typical density profile is the solution of the differential equation (see SVMS and references therein)

$$\frac{d\delta_{pk}}{dR_f} = -x_e(R_f, \delta_{pk}) \sigma_2(R_f) R_f, \quad (10)$$

where $\sigma_2(R_f)$ is the second order spectral moment and the inverse of $x_e(R_f, \delta_{pk})$ is the average inverse curvature x (minus the Laplacian over σ_2) of peaks with density contrast δ_{pk} at the scale R_f (see SVMS for the explicit form of these two functions). Equation (10) can be solved for the boundary condition $\delta_{pk}[R_f(M)] = \delta(t)$ leading to the halo with M at t according to the one-to-one correspondence between peaks and haloes given by (Manrique & Salvador-Solé 1995)

$$R_f(M) = \frac{1}{q} \left[\frac{3M}{4\pi \bar{\rho}(t_i)} \right]^{1/3}, \quad (11)$$

and

$$\delta(t) = \delta_c(t) \frac{G(t_i)}{G(t)} \quad (12)$$

where q is the radius, in units of R_f , of the collapsing cloud with volume equal to $M/\bar{\rho}(t_i)$ associated with the peak, $G(t)$

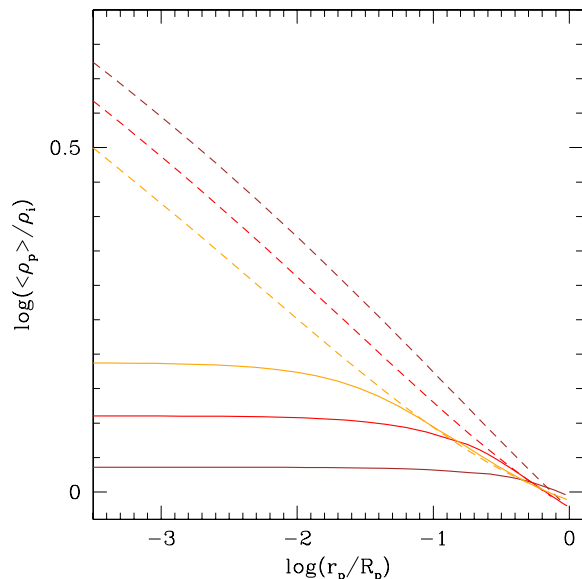


Figure 2. Spherically averaged (unconvolved) density profile for the same halo seeds and cosmologies as in Figure 1 (same lines).

is the cosmic growth factor and $\delta_c(t)$ is the critical linearly extrapolated density contrast for spherical collapse at t . In the underlying Λ CDM cosmology here considered, such a correspondence is given by $q = 2.75$ and $\delta_c(z) = 1.82 + (6.03 - 0.472z + 0.0545z^2)/(1 + 0.000552z^3)$ where z is the redshift corresponding to t .⁴

The peak trajectories, $\delta_{pk}(R_f)$, solution of equation (10) in the WDM (CDM) cosmology for current haloes with three relevant masses are shown in Figure 1. As can be seen, the $\delta_{pk}(R_f)$ trajectories in the WDM cosmology level off, contrarily to those in the CDM cosmology, at some value δ_{fs} that depends on the halo mass. The time t_{fs} corresponding to δ_{fs} (eq. [12]) marks the time when the first ancestor of the halo with a given current mass M forms and initiates the continuous series of ancestors leading by PA to that final halo. Before that time there is no ancestor of haloes with that current mass in the WDM cosmology. Instead, there are halo ancestors down to any arbitrarily small time in the CDM cosmology, with no spectrum cut-off.

In Figure 2, we show the spherically averaged density profile, $\langle \rho_p \rangle(r_p)$, of WDM (and CDM) halo seeds resulting from equation (9) for the peak trajectories depicted in Figure 1. As can be seen, contrarily to their CDM counterparts, the WDM halo seeds show apparent flat cores with a universal mass very approximately equal to the mass $M_{fs} = [4\pi/3] \bar{\rho}(t_0) (\lambda_{fs}^{eff}/2)^3 = 6.5 \times 10^5 M_\odot$ associated with the effective free-streaming scale length $\lambda_{fs}^{eff} \equiv 2\pi/k_{fs}^{eff} = \alpha$. Note that this is different from the mass associated with scale length equal to 2π over the wavenumber where $T_{fs}^2(k)$ decreases to 0.5, also often used to estimate the free-streaming mass. This latter scale length is substantially greater than α , so it would correspond to the scale length where the effects of WDM begin to be noticeable rather than the minimum size of density perturbations. For this reason, following Schnei-

⁴ This yields the right halo mass function at every redshift (see Manrique & Salvador-Solé 1995).

der et al. (2011), the mass $\sim 1.8 \times 10^9 M_\odot$ associated with it will be called the half-mode mass, M_{hm} .

If the velocity dispersion in the seed were negligible, its flat core with mass $\sim M_{\text{fs}}$ would expand and collapse at once, with no shell-crossing before turnaround⁵. Consequently, these flat protohalo cores with mass $\sim M_{\text{fs}}$ set a lower bound for the mass of WDM haloes. In contrast, there are no flat cores in the CDM cosmology, so there is no lower bound for the mass of CDM haloes either. One can find ancestors of any accreting halo with M at t down to arbitrarily small cosmic times and with arbitrarily low masses.

4 WDM HALO DENSITY PROFILE

The lower-bound mass, M_{fs} , for haloes in the WDM cosmology just mentioned arises from the spectrum cutoff. But this bound mass has been obtained by neglecting the WDM particle velocity dispersion, σ_{DM} . Actually, the non-negligible velocity dispersion of WDM particles causes the total energy $E_{\text{p}}(R_{\text{p}})$ in the seed (eq. [5]) to become positive for radii R_{p} below some value R_{E} . This means that shells inside that radius, with velocity dispersion larger than the Hubble velocity, expand more rapidly than outer ones, which causes the system to run out of linear regime, leading to the formation of caustics. These caustics will fragment (owing to the perturbation of the surrounding matter) and give rise to small nodes with masses substantially less than $M_{\text{E}} \equiv M(R_{\text{E}})$, the mass of that part of the seed with null total energy. This means that haloes with masses below $M_{\text{E}} > M_{\text{fs}}$ do not actually evolve in the bottom-up fashion and that the typical WDM halo density profile will not satisfy equation (4) at radii enclosing M_{E} .

According to Boyanovsky et al. (2008), the value of σ_{DM} today for non-thermal sterile neutrinos is related to the free-streaming wavenumber through

$$k_{\text{fs}}^{\text{eff}} \approx \left[\frac{3H^2(t_0)\Omega_{\text{M}}}{2\sigma_{\text{DM}}^2(t_0)} \right]^{1/2}. \quad (13)$$

In the present case, this leads to $\sigma_{\text{DM}}(t_0) = 0.23 \text{ km s}^{-1}$. This value is markedly greater than the one usually adopted in this kind of studies⁶, which might overestimate the effects of the velocity dispersion on the predicted structure of WDM haloes. For this reason, we will be more conservative. We will adopt $\sigma_{\text{DM}}(t_0) = 0.075 \text{ km s}^{-1}$ and study the effects of changing the value of $\sigma_{\text{DM}}(t_0)$ by comparing the density profiles so obtained (WDMNT model) with those arising from a null value of $\sigma_{\text{DM}}(t_0)$ (WDM0 model), so to see the effects of the cutoff in the spectrum alone, as well as a value of $\sigma_{\text{DM}}(t_0)$ equal to that of thermal neutrino-like WDM particles (WDMT model). According to Steffen

⁵ In fact, these shells would not cross each other even after turnaround, meaning that such a flat perturbation would oscillate for ever and would not virialise. However, the subsequent shells coming from outside the flat core do cross them and the system finally virialises.

⁶ Colín et al. 2008 take $\sigma_{\text{DM}}(t_0)$ equal to 3 times the thermal velocity dispersion.

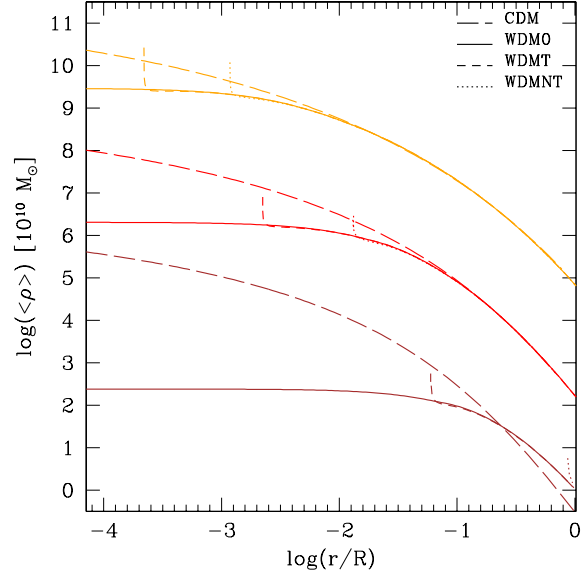


Figure 3. Typical spherically averaged density profiles predicted for current haloes with the same masses and in the same cosmologies (same colours) as in the previous Figures: Λ WDM cosmology with null velocity dispersion (WDM0; solid lines), with thermal velocity dispersion (WDMT; short-dashed lines) and with non-thermal velocity dispersion (WDMNT; dotted lines); Λ CDM cosmology (CDM long-dashed lines). To avoid crowding the profiles corresponding to $10^9 M_\odot$ and $10^{13} M_\odot$ have been shifted 2.5 dex downwards and upwards, respectively.

(2006), this latter velocity dispersion is given by,

$$\sigma_{\text{DM}}^3(t_0) = 0.041^3 \left(\frac{h}{0.7} \right)^2 \left(\frac{m_{\text{WDM}}}{1 \text{ keV}} \right)^{-4} \frac{\Omega_{\text{WDM}}}{0.25} (\text{km s}^{-1})^3, \quad (14)$$

leading for 2 keV particles to $\sigma_{\text{DM}}(t_0) = 0.015 \text{ km s}^{-1}$. The reference Λ CDM halo profiles are derived assuming, of course, a negligible $\sigma_{\text{DM}}(t_0)$.

In Figure 3, we plot the typical spherically averaged halo density profiles for current haloes with the same masses as used in the previous Figures, each of them for the three values of $\sigma_{\text{DM}}(t_0)$ just mentioned. All the profiles deviate from the corresponding CDM halo profiles in the same monotonous way leading to a flat core with mass M_{fs} . However, the only profile that can be strictly traced down to the halo centre is the WDM0 profile. The remaining profiles (for non-vanishing $\sigma_{\text{DM}}(t_0)$) show a sharp up-turn to infinity at a small enough radius. This reflects the fact that, for M approaching the value M_{E} where $E_{\text{p}}(M)$ vanishes (eq. [5]), equation (4) is no longer valid. For thermal velocity dispersion (WDMT profile), the minimum radius reached essentially coincides with the edge of the flat core, while, for larger values of $\sigma_{\text{DM}}(t_0)$, it is significantly larger. The mass M_{E} encompassed by the minimum radius reached in the case of non-thermal velocity dispersion (WDMNT profile), of the order of the half-mode mass, M_{hm} , for the value of $\sigma_{\text{DM}}(t_0)$ used here, shows a slight trend to diminish with increasing halo mass. Specifically, it is equal to $10^9 M_\odot$, $1.9 \times 10^8 M_\odot$ and $8.1 \times 10^7 M_\odot$ for haloes with $10^9 M_\odot$, $10^{11} M_\odot$ and $10^{13} M_\odot$, respectively.

5 CONCLUSIONS

The typical spherically averaged density profile for haloes with masses greater than the free-streaming mass, M_{fs} , in the WDM cosmology can be derived analytically by means of the SVMS model. As a consequence of the spectrum cutoff, the density profiles so obtained show a clear flattening relative to the profiles found in CDM cosmologies, independent of the particle velocity dispersion, which gradually evolves into a flat core with mass equal to M_{fs} . A particle mass as low as 2 keV is enough for the flattening to begin to be visible, at a radius of ~ 0.005 virial radii as reached in current N -body simulations, for haloes with masses M as large as $\sim 10^{13} M_{\odot}$ and the flat core is already reached, at those radii, for haloes with $M \lesssim 10^{11} M_{\odot}$.

The only apparent effect of the particle velocity dispersion is that it prevents from reaching the flat core. In fact, such a core might not exist, that is the density profile at the halo centre might not be flat. Indeed, the velocity dispersion causes protohaloes to have null total energy within some small radius encompassing the mass M_{fs} . This produces caustics as protohaloes expand, leading to their fragmentation into small nodes. This would explain the presence of haloes with masses below M_{fs} in N -body simulations of WDM cosmologies. Therefore, small mass haloes do not grow in the bottom-up hierarchical fashion and their density profile cannot be recovered by means of the SVMS model. For a 2 keV particle mass and a non-thermal velocity dispersion of $\sim 0.075 \text{ km s}^{-1}$, the “unresolved core” affects the whole density profile for haloes with masses below $\sim 10^9 M_{\odot}$. The larger the velocity dispersion, the larger the minimum radius that can be reached in the density profile of any given halo. All these effects are obviously relaxed for increasing particle masses, which cannot be ruled out according to the present results.

ACKNOWLEDGEMENTS

This work was supported by the Spanish DGES, AYA2009-12792-C03-01, and the Catalan DIUE, 2009SGR00217. One of us, JV, was beneficiary of a Spanish FPI grant.

REFERENCES

- Bento M. C., Bertolami O., Rosenfeld R., 2000, *Phys. Rev. D*, 62, 041302(R)
- Boyanovsky D., de Vega H.J., Sanchez N.G., 2008, *Phys. Rev. D*, 78, 063546
- Boyarsky A., Lesburgues J., Ruchayskiy O., Viel M., 2009, *Phys. Rev. Lett.*, 102, 201304
- Boylan-Kolchin M., Bullock J. S., Kaplinghat M., 2011, *MNRAS*, 415, L40
- Cole S., Percival W. J., Peacock J. A., Norberg P., Baugh C. M., Frenk C. S., Baldry I., Bland-Hawthorn J., and 23 others, 2005, *MNRAS*, 362, 505
- Colín P., Avila-Reese V., Valenzuela O., 2000, *ApJ*, 539, 561
- Colín P., Valenzuela O., Avila-Reese V., 2008, *ApJ*, 673, 203
- Ellis J., Hagelin J. S., Nanopoulos D. V., Olive K., Srednicki M., 1984, *Nucl. Phys. B*, 238, 453
- Goerdt T., Moore B., Read J. I., Stadel J., Zemp M., 2006, *MNRAS*, 368, 1073-1077
- Gorbunov D., Khmelnitsky A., Rubakov V., 2008, *JHEP*, 12 55
- Hogan C.J., Dalcanton J.J., 2000, *Phys. Rev. D*, 42, 3329
- Kaplinghat M., Knox L., Turner, M. S., 2000, *Phys. Rev. Lett.*, 85, 3335
- Kaplinghat M., 2005, *Phys. Rev. D*, 72, 063511
- Klypin A.A., Kravtsov A.V., Valenzuela O., Prada F., 1999, *ApJ*, 522:82-92
- Knebe A., Devriendt J., Mahmood A., Silk J., 2002, *MNRAS*, 329, 813
- Komatsu E., Smith K. M., Dunkley J., Bennet C. L., Gold B., Hinshaw G., Jarosik N., Larson D., and 13 others, 2011, *ApJS*, 192, 18
- Manrique A. & Salvador-Solé E., 1995, *ApJ*, 453, 6
- Salvador-Solé E., Viñas, J., Manrique A., Serra S., 2012, submitted to *MNRAS* (SVMS)
- Shaposhnikov M. & Tkachev I., 2006, *Phys. Lett. B*, 639, 414
- Spergel, D. N., Steinhart P. J., 2000, *Phys. Rev. Lett.*, 84, 3760
- Steffen F. D., 2006, *Journal of Cosmology and Astro-Particle Physics*, 9, 1
- Viel M., Lesburgues J., Haehnelt M. G., Matarrese S., Riotto A., 2005, *Phys.Rev.D*, 71, 063534
- Wang J. & White S. D. M., 2009, *MNRAS*, 396, 709
- Wang J. & White S. D. M., 2007, *MNRAS*, 380, 93